SLAC-PUB-13024
UCHEP-07-09

D^0- $\overline{D}^0$ Mixing Analyses at *BABAR*

Rolf Andreassen* (for the *BABAR* collaboration)
University of Cincinnati, Cincinnati, Ohio 45221, USA
(Dated: December 5, 2007)

We summarise results of analyses of D meson mixing parameters performed by the *BABAR* collaboration.

PACS numbers: 14.40.Lb, 12.15.Ff

INTRODUCTION

Understanding D meson (charm) mixing is an important step in measuring *CP* violation in the charm sector. It also fills in a gap between the well-measured cases of K [1] and B [2, 3] system mixing, both of which have down-type quarks in the intermediate state, where charm mixing has up-type quarks. Since mixing in the D^0 system is expected to be small in the Standard Model [4] (modulo the hard-to-predict effects of long-distance interactions [5]), charm mixing also offers a chance to observe New Physics either through *CP* violation in mixing [10] or a large mass difference between the D mass eigenstates [5]. In this proceeding, we summarise the result of four different approaches to measuring the D mixing parameters at *BABAR*, involving the decays $D^0 \to K^+ \pi^-$ [6], $D^0 \to K^+ K^-$ or $\pi^+ \pi^-$ [7], $D^0 \to K^+ \pi^- \pi^0$ [8], and $D^0 \to K^+ \pi^- \pi^+ \pi^-$ [9].

DETECTOR

We present analyses of e^+e^- collisions at a center-of-mass (CM) energy of 10.58, collected at the *BABAR* detector at the PEP-II storage ring. Particle identification is done by dE/dx measurements from two tracking detectors and from measuring Cherenkov angles in a ring-imaging detector. D mesons are tagged by reconstructing $D^{*+} \to D^0 \pi^+$ and $D^{*-} \to \overline{D}^0 \pi^-$ decays, and assigning flavour according to the charge of the slow pion.

FORMALISM AND NOTATION

D mesons are produced in pure flavour eigenstates, $|D^0\rangle$ or $|\overline{D}^0\rangle$. These flavour eigenstates are not equal to the mass and lifetime eigenstates

$$\begin{aligned} |D_1\rangle &= p|D^0\rangle + q|\overline{D}^0\rangle \\ |D_2\rangle &= p|D^0\rangle - q|\overline{D}^0\rangle \end{aligned}$$

by which they propagate and decay. Therefore, a particle produced as a D^0 may become a $\overline{D}^0$ before its decay. The process is governed by the mass and lifetime differences of the D_1 and D_2 states; these decay according to

$$\begin{aligned} |D_1(t)\rangle &= e^{-i(m_1 - i\Gamma_1/2)t}|D_1\rangle \\ |D_2(t)\rangle &= e^{-i(m_2 - i\Gamma_2/2)t}|D_2\rangle \end{aligned}$$

where m_i, Γ_i are the mass and width of the D_i state. We define

$$\begin{aligned} \Delta M &= m_1 - m_2 \\ \Delta\Gamma &= \Gamma_1 - \Gamma_2 \\ \Gamma &= (\Gamma_1 + \Gamma_2)/2 \\ x &= \Delta M/\Gamma \\ y &= \Delta\Gamma/2\Gamma \\ R_M &= (x^2 + y^2)/2 \end{aligned}$$

The quantities x and y are collectively referred to as mixing parameters. Estimates within the Standard Model vary from 10^{-4} (counting only short-distance effects) to as high as 1%. Establishing the presence of New Physics requires either $x >> y$, or *CP* violation [5].

EXPERIMENTAL APPROACH

The studies considered here use a common apparatus for tagging D mesons as either D^0 or $\overline{D}^0$, and for measuring their decay times. In particular, by considering only D mesons from $D^* \to D^0 \pi_s$, we can use the charge of the slow pion π_s to determine the production flavour of the D^0, and measure its flight length from the decay vertices of the D^* and D^0 particles.We make use of the mass of D^0 candidates (m_{D^0}) and the mass difference Δm between D^0 and D^* candidates to extract our signal yields, and to define sidebands for background studies. Figure 1 shows distributions of these quantities for the $D^0 \to K^- \pi^+$ analysis, which may be considered typical.

For historical reasons, D mesons whose decay flavour matches their production flavour (e.g. $D^{*+} \to D^0 \pi^+$ with $D^0 \to K^- \pi^+$) are called 'right-sign' (RS), while the opposite case is referred to as 'wrong-sign' (WS).

*Email:rolfa@slac.stanford.edu

Invited talk presented at International Conference On Hadron Spectroscopy (Hadron 07), 10/8/2007-10/13/2007, Frascati, Italy
Work supported in part by US Department of Energy contract DE-AC02-76SF00515

Wrong-sign decays may come about either through mixing or through doubly-Cabibbo-suppressed (DCS) Feynmann diagrams. To distinguish the two cases, we use the decay-time distribution, as will be shown for each decay mode.

In addition to these two sources of wrong-sign events, there is the case where a correctly reconstructed D^0 is matched with a pion not from a D^* decay to produce a spurious D^*; this is referred to as the "mistag" background. Another source of background is D mesons reconstructed with the correct tracks, but wrong particle assigments, or with tracks missing; this is the "bad D^0" or "mis-reconstructed charm" background. Finally there is background from combinatorics.

$$\boldsymbol{D^0 \to K^+ \pi^-}$$

In the limit of small mixing and *CP* conservation, the decay-time distribution for wrong-sign decays of mesons produced as D^0 may be approximated as

$$\frac{T_{\rm WS}(t)}{e^{-\Gamma t}} \propto R_D + y'\sqrt{R_D}(\Gamma t) + \frac{1}{4}(x'^2 + y'^2)(\Gamma t)^2 \quad (1)$$

where x' and y' are related to x and y by

$$\begin{aligned} x' &= x\cos\delta_{K\pi} + y\sin\delta_{K\pi} \\ y' &= y\cos\delta_{K\pi} - x\sin\delta_{K\pi}. \end{aligned}$$

The angle $\delta_{K\pi}$ is the strong phase between Cabibbo-favoured (CF) and DCS decays. The quantity R_D is the amplitude, in the absence of mixing, for the D^0 to decay by a DCS process; the term quadratic in t is the amplitude, in the absence of DCS processes, for the D^0 to mix and then decay as a $\overline{D}^0$; and the term linear in t is the interference term between these two processes.

We apply Equation 1 in two ways: The first is to enforce *CP* conservation by fitting both D^0 and $\overline{D}^0$ samples together. The second is to search for *CP* violation by doing two fits, calculating x'^2 and y' for D^0 and $\overline{D}^0$ separately.

We use 384 fb^{-1} of e^+e^- data, pairing tracks of opposite charge to make D^0 candidates, and then pairing these with slow pion tracks to make D^* candidates. The phase space available for slow pions is small; we require their momentum to be greater than 0.1 GeV/c in the lab frame, and less than 0.45 GeV/c in the CM frame. We fit the full decay chain, constraining the D^* to come from the beam spot, the D^0 and slow pion to come from a common vertex, and the $K^\mp$ and $\pi^\pm$ to come from a different common vertex. We reject candidates if the χ^2 probability of this fit is less than 0.1%. The D^0 decay time and error on the decay time are taken from this fit; candidates whose decay-time error exceeds 0.5 ps are assumed to be badly reconstructed, and thrown away, and we also require that the decay time be between -2 and 4 ps. We further require the CM momentum of D^0 candidates to be at least 2.5 GeV/c, which suppresses backgrounds from B-meson decays and combinatorics. Where multiple D^* candidates share tracks, we use only the candidate with the highest χ^2 probability from the fit. With these criteria, our samples consist of 1,229,000 RS and 64,000 WS D^0 and $\overline{D}^0$ candidates. Figure 1 shows their distribution in $m_{K\pi}$ and Δm.

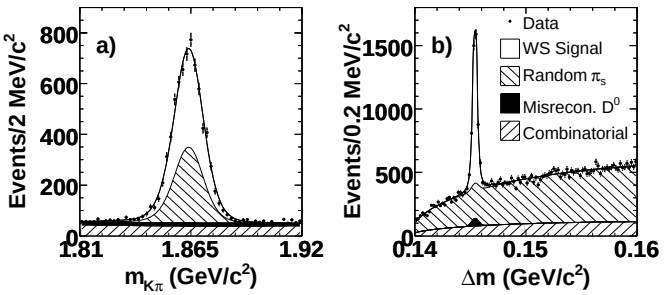

FIG. 1: a) $m_{K\pi}$ for wrong-sign (WS) candidates with $0.1445 < \Delta m < 0.1465\,\mathrm{GeV}/c^2$, and b) Δm for WS candidates with $1.843 < m_{K\pi} < 1.883\,\mathrm{GeV}/c^2$. The fitted PDFs are overlaid.

We extract the mixing parameters using an unbinned, extended maximum-likelihood fit, which proceeds in three stages. The first step is to fit the $m_{K\pi} - \Delta m$ distributions to extract shape parameters in these variables; these are then fixed in subsequent fits. Next we fit the RS sample to extract the D^0 lifetime and resolution functions, using the $m_{K\pi} - \Delta m$ parameters from the previous step to separate the components. Finally we fit the WS sample for the mixing parameters using three different models. The first model assumes no *CP* violation and no mixing; the second permits mixing, but not *CP* violation; the third allows both mixing and *CP* violation.

The $m_{K\pi} - \Delta m$ distributions are fitted to a sum of four PDFs, one each for signal, mistags, bad D^0 and combinatorial background. Of these, the signal peaks in both $m_{K\pi}$ and Δm. The mistagged events - correctly reconstructed D^0 with a pion not from a D^* decay - peak in $m_{K\pi}$ but not in Δm. Bad D^0 events have a D^0 with one or more daughters missing, or assigned the wrong particle hypothesis; they peak in Δm but not in $m_{K\pi}$. Finally, combinatorial background does not peak in either variable. Figure 1 shows these various shapes. The signal peak contains $1,141,500 \pm 1,200$ candidates for the RS sample, and $4,030 \pm 90$ for the WS.

We describe the decay-time distribution of the RS signal with an exponential convolved with a sum of three Gaussians, whose widths are proportional to the measured event-by-event error on the decay time. The combinatorial background is described by a sum of two Gaussians, one of which has a power-law tail; the mistag background is described by the same PDF as the signal, because the slow pion has little influence on the vertex fit.

For the WS signal, we use Equation 1, convolved with the resolution function determined by the RS fit. Figure 2 shows the data, overlaid by these various PDFs. From inspection, it is clear that the fit allowing mixing describes the data better than the one which imposes zero mixing.

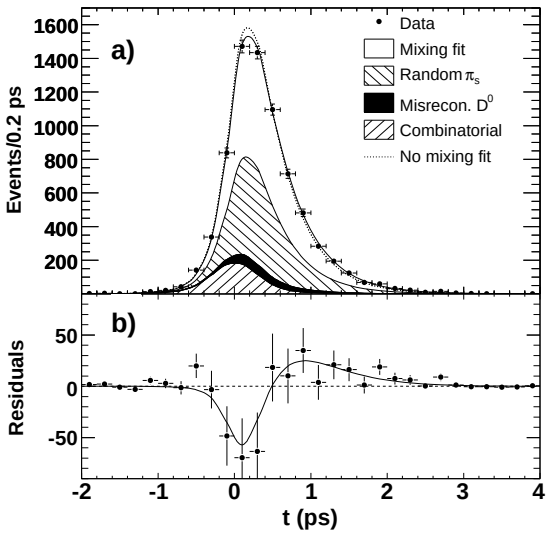

FIG. 2: a) Projections of the proper-time distribution of combined D^0 and $\overline{D}^0$ WS candidates and fit result integrated over the signal region $1.843 < m_{K\pi} < 1.883$ GeV/c^2 and $0.1445 < \Delta m < 0.1465$ GeV/c^2. The result of the fit allowing (not allowing) mixing but not *CP* violation is overlaid as a solid (dashed) curve. b) The points represent the difference between the data and the no-mixing fit. The solid curve shows the difference between fits with and without mixing. The difference between the mixing-allowed fit and the data is therefore the difference between the solid curve and the points, or essentially zero.

Figure 3 shows the likelihood contours of the mixing parameters from the fit allowing mixing but not *CP* violation, including systematic uncertainties. The point of maximum probability is in the unphysical region where x'^2 is negative; adjusting for this by moving to the most likely point in the physical region, $x'^2 = 0$, $y' = 6.4 \times 10^{-3}$, we find that $-2\Delta \ln \mathcal{L}$ is 23.2 units between the most likely physical point and the point of no mixing. Including the systematic uncertainties, we thus find mixing at a significance of 3.9 σ. Table I shows the results of our fits in more detail; we find no evidence for *CP* violation, as shown by the asymmetry $A_D = (R_D^+ - R_D^-)/(R_D^+ + R_D^-)$ where subscript '+' indicates only the D^0 sample was used, and '−' indicates the $\overline{D}^0$ sample.

We evaluate systematic uncertainties from three sources: Variations in the fit model, in the selection criteria, and in our procedure for dealing with track-sharing D^* candidates. The most significant source of systematic uncertainty in R_D and the mixing parameters is from the fit model for the long-lived background component

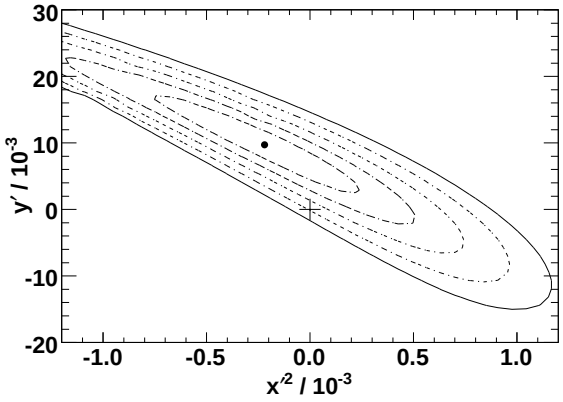

FIG. 3: The central value (point) and confidence-level (CL) contours for $1 - \mathrm{CL} = 0.317$ (1σ), 4.55×10^{-2} (2σ), 2.70×10^{-3} (3σ), 6.33×10^{-5} (4σ) and 5.73×10^{-7} (5σ), calculated from the change in the value of $-2 \ln \mathcal{L}$ compared with its value at the minimum. Systematic uncertainties are included. The no-mixing point is shown as a plus sign (+).

TABLE I: Results from the different fits. The first uncertainty listed is statistical and the second systematic.

Fit type	Parameter	Fit Results ($/10^{-3}$)
No *CP* viol. or mixing	R_D	$3.53 \pm 0.08 \pm 0.04$
No *CP* violation	R_D	$3.03 \pm 0.16 \pm 0.10$
	x'^2	$-0.22 \pm 0.30 \pm 0.21$
	y'	$9.7 \pm 4.4 \pm 3.1$
CP violation allowed	R_D	$3.03 \pm 0.16 \pm 0.10$
	A_D	$-21 \pm 52 \pm 15$
	x'^{2+}	$-0.24 \pm 0.43 \pm 0.30$
	y'^{+}	$9.8 \pm 6.4 \pm 4.5$
	x'^{2-}	$-0.20 \pm 0.41 \pm 0.29$
	y'^{-}	$9.6 \pm 6.1 \pm 4.3$

caused by other D decays in the signal region, followed by the presence of a non-zero mean in the time-resolution function, caused by small misalignments in the detector. For the asymmetry A_D, the dominant contribution is uncertainty in modeling the differences between K^+ and K^- absorption in the detector.

$D^0 \to K^+K^-$ OR $\pi^+\pi^-$

For D mesons decaying to *CP* eigenstates, mixing changes the decay time distribution in such a way that we may, to a good approximation, consider the decays exponential with changed lifetimes ([11])

$$\tau^+ = \tau^0 \left[1 + |q/p| \left(y \cos\phi_f - x \sin\phi_f\right)\right]^{-1}$$
$$\tau^- = \tau^0 \left[1 + |p/q| \left(y \cos\phi_f + x \sin\phi_f\right)\right]^{-1}$$

where τ^0 is the lifetime for decays to final states which are not *CP* eigenstates, and τ^+ (τ^-) is the lifetime for

D^0 ($\overline{D}^0$) decays to *CP*-even states. We can combine the three lifetimes into quantities

$$\begin{aligned} y_{CP} &= \tau^0/\langle\tau\rangle - 1 \\ \Delta Y &= \left(\tau^0 A_\tau\right)/\langle\tau\rangle. \end{aligned}$$

Here ϕ_f is the *CP*-violating phase $\phi_f = \arg(q\overline{A}_f/pA_f)$, A_f ($\overline{A}_f$) being the amplitude for D^0 ($\overline{D}^0$) decaying to the final state f. $\langle\tau\rangle$ is the average of τ^+ and τ^-, and A_τ is their asymmetry $(\tau^+ - \tau^-)/(\tau^+ + \tau^-)$. In the absence of mixing, both y_{CP} and ΔY are zero. In the absence of *CP* violation in the interference of mixing and decay (ie, $\phi_f = 0$), ΔY is zero and $y_{CP} = y$.

For this analysis, we use 384 fb^{-1} of *BABAR* data, and measure the lifetimes for the *CP*-even decays[1] $D^0 \to K^+ K^-$ and $D^0 \to \pi^+ \pi^-$, and for $D^0 \to K^- \pi^+$, which is not a *CP* eigenstate and thus gives our τ^0.

In addition to particle identification requirements, the cosine of the helicity angle (defined as the angle between the momentum of the positively charged D^0 daughter in the D^0 rest frame, and the D^0's momentum in the lab frame) is required less than 0.7; this suppresses combinatorial backgrounds. D^0 candidates are then combined with pions to produce D^* candidates. Electrons are rejected by combining pion candidates with each other track in the event and vetoing those which form a good photon conversion or pion Dalitz decay, as well as by $\mathrm{d}E/\mathrm{d}x$ measurements. The requirements for slow pions and the vertex fit of the D^* are the same as for the $D^0 \to K^- \pi^+$ analysis (Section 5).

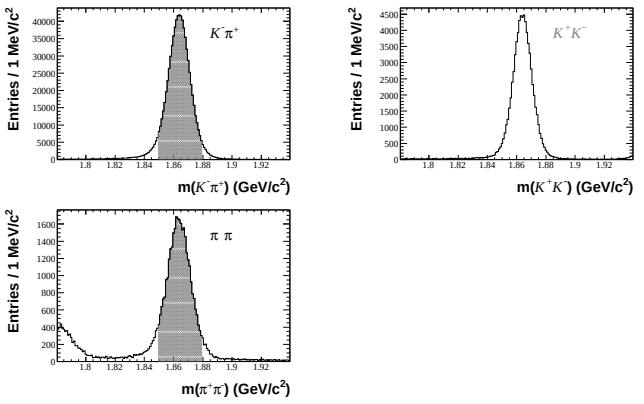

FIG. 4: Reconstructed D^0 mass distributions for the three D^0 samples, within ± 0.8 MeV/c^2 of the Δm peak.

Figure 4 shows the mass distributions of D^0 candidates; Table II shows the yield and purity of the samples, calculated using events within a 15 MeV/c^2 D^0 mass and 0.8 MeV/c^2 Δm window. We fit the decay time distributions of these samples using an unbinned maximum likelihood fit to all five decay modes simultaneously, using separate PDFs for signal decays, mistagged events, mis-reconstructed charm events, and combinatorial background.

Sample	Size	Purity (%)
$K^-\pi^+$	730,880	99.9
K^-K^+	69,696	99.6
$\pi^-\pi^+$	30,679	98.0

TABLE II: Sample sizes and purities.

As with the $D^0 \to K^- \pi^+$ study, we model the decay-time distribution of signal events using a simple exponential convolved with a sum of three Gaussians for the resolution. Each Gaussian has a width proportional to the event-by-event error on the measured decay time; their mean is common, and allowed to be offset from zero to account for any effects of detector mis-alignment. Mistagged events - that is, events with a correctly reconstructed D^0, but wrongly assigned slow pion - account for about 0.4% of the sample; of these, half will have the wrong flavour assignment to the D^0. However, they have the same decay-time distribution and resolution as true signal. Hence we model these events using the signal PDF, but reversing the flavour assignment.

Mis-reconstructed charm events have an exponential decay-time distribution, which we convolve with a single Gaussian. The fraction of such events is obtained from simulation, which we check by comparing data and Monte Carlo in the sidebands $1.89 < m_{D^0} < 1.92\,\mathrm{GeV}/c^2$ and $0.151 < \Delta m < 0.159\,\mathrm{GeV}/c^2$. We estimate the charm background as $(0.009 \pm 0.002)\%$ of events in the signal region for $D^0 \to K^- \pi^+$, $(0.2 \pm 0.1)\%$ for $D^0 \to K^+ K^-$, and $(0.15 \pm 0.15)\%$ for $D^0 \to \pi^+ \pi^-$. For combinatorial background, we model the decay-time distribution as the sum of a Gaussian and a modified Gaussian with a power-law tail, the latter accounting for a long-lived component. Each decay mode has its own shape for combinatorial background, the shapes being determined from fits to the sideband regions; the fraction of this background is again estimated from Monte Carlo with uncertainties derived from comparison of MC and data. We find $(0.032 \pm 0.003)\%$ in the $D^0 \to K^- \pi^+$ mode, $(0.16 \pm 0.02)\%$ in $D^0 \to K^+ K^-$, and $(1.8 \pm 0.2)\%$ in $D^0 \to \pi^+ \pi^-$.

We consider several sources of systematic error, including variations of the signal and background models, changes to the event selection, and detector effects. We vary the models by changing the signal PDF shape and size, as well as the position of the signal box. We also test our resolution model by forcing the common mean of the three Gaussians to zero, and by allowing it to float separately for different bins of the D^0 polar angle. Of

[1] Charge conjugation is implied throughout unless otherwise noted.

TABLE III: Summary of systematic uncertainties on y_{CP} and ΔY, separately for KK and $\pi^+\pi^-$ and averaged over the two CP modes, in percent.

	$\sigma_{y_{CP}}$ (%)			$\sigma_{\Delta Y}$ (%)		
Systematic	KK	$\pi^+\pi^-$	Avg.	KK	$\pi^+\pi^-$	Avg.
Signal model	0.130	0.059	0.085	0.072	0.265	0.062
Charm bkg	0.062	0.037	0.043	0.001	0.002	0.001
Comb. bkg	0.019	0.142	0.045	0.001	0.005	0.002
Selection criteria	0.068	0.178	0.046	0.083	0.172	0.011
Detector model	0.064	0.080	0.064	0.054	0.040	0.054
Quadrature sum	0.172	0.251	0.132	0.122	0.318	0.083

these effects, the largest systematic uncertainty derives from widening the D^0 mass window, which increases the amount of badly-reconstructed signal events in the sample.

We vary the mis-reconstructed charm model by changing its fraction in the fit, by varying its effective lifetime, by using a different sideband region, and by using a decay time distribution obtained from Monte Carlo instead of the sideband data. Due to the purity of the data, these effects are all small, the largest being from varying the background fraction in the $D^0 \to \pi^+\ \pi^-$ mode, where the purity is worst.

We vary our event selection criteria in two ways: By throwing out or keeping all multiple candidates (as opposed to selecting the candidate with the best χ^2 probability for its vertex fit), and by changing the acceptable range of errors on decay times. The last, which changes the amount of poorly reconstructed signal events, has the largest effect.

Finally, we consider effects of our understanding of the detector by repeating our analysis with different misalignment parameters. This changes our fitted lifetimes by up to 3 fs; but since the lifetimes change by similar amounts, and we are considering ratios of lifetimes, the effect on the mixing parameters is small. All these systematic effects are summarised in Table III.

The results of these decay-time fits are shown in Table IV. From the measured lifetimes, we extract

$$\begin{aligned} y_{CP} &= 1.24 \pm 0.39(\text{stat}) \pm 0.13(\text{syst})]\% \\ \Delta Y &= [-0.26 \pm 0.36(\text{stat}) \pm 0.08(\text{syst})]\% \end{aligned}$$

Mode	Lifetime (fs)
$D^0 \to K^-\ \pi^+$	409.33 ± 0.70
$D^0\ (D^{*+}) \to K^+\ K^-$	401.28 ± 2.47
$D^0\ (D^{*-}) \to K^+\ K^-$	404.47 ± 2.52
$D^0\ (D^{*+}) \to \pi^+\ \pi^-$	407.64 ± 3.68
$D^0\ (D^{*-}) \to \pi^+\ \pi^-$	407.26 ± 3.73

TABLE IV: Measured lifetimes for the different decay modes. Uncertainties are statistical only.

which is evidence for D^0-$\overline{D}^0$ mixing at the 3-sigma level, and consistent with CP conservation. This amount of D^0-$\overline{D}^0$ mixing is consistent with Standard Model predictions.

$D^0 \to K^+\ \pi^-\ \pi^0$

For the case of D^0 decays to three-body final states, we can modify Equation 1 to give a decay-time distribution for each point in the decay phase space:

$$\begin{aligned} \mathcal{A}(P,t) \;=\; & e^{-\Gamma t}\Big[|\overline{A_P}|^2 \\ & +|\overline{A_P}||A_P|\,(y''\cos\delta_P - x''\sin\delta_P)\,\Gamma t \\ & +|A_P|^2(x''^2+y''^2)(\Gamma t)^2\Big]. \end{aligned} \tag{2}$$

In analogy with Equation 1, $\overline{A_P}$ is the amplitude (in the absence of mixing) for D^0 mesons to decay by a DCS process to the point P on the Dalitz plot. The term quadratic in time is the amplitude (in the absence of DCS processes) for the D^0 to mix before its decay, and then decay to the point D by a CF process. Within this term, the factor A_P is the amplitude for the CF decay, while the remaining factors are the mixing amplitude. The term linear in time is the interference between the DCS and mixing terms. The quantity δ_P is the phase of the intermediate states in the decay, relative to some reference resonance. As with the $D^0 \to K^-\ \pi^+$ case, an unknown strong phase $\delta_{K\pi\pi^0}$ between CF and DCS decays prevents us measuring x and y directly; instead we are sensitive to

$$\begin{aligned} x'' &= x\cos\delta_{K\pi\pi^0} + y\sin\delta_{K\pi\pi^0} \\ y'' &= y\cos\delta_{K\pi\pi^0} - x\sin\delta_{K\pi\pi^0}. \end{aligned}$$

As with the previous two analyses, we use 384 fb^{-1} of *BABAR* data, reconstructing $D^0 \to K^-\ \pi^+\ \pi^0$ candidates from two oppositely-charged tracks and two photon candidates with energy at least 100 MeV. The π^0 candidate is required to have a lab momentum of at least 350 MeV/c, and a mass-constrained fit probability of at least 1%. The slow pion is required to have a momentum transverse to the beam axis of at least 120 MeV/c, and the D^0 candidate to have a CM momentum of at least 2.4 GeV/c. As in the previous two analyses, we extract the D^0 decay time, with error, from a vertex fit constraining the D^* to the beam spot; this fit is required to have a χ^2 probability of at least 1%.

Figure 5 shows the $m_{K\pi\pi}$ and Δm distributions that result from these criteria. We fit these distributions as described for the $D^0 \to K^-\ \pi^+$ study in Section 5; the fit to the WS sample uses shape parameters from the RS fit, suppressing the associated systematics. Table V shows the yields for each component.

We compute the quantity A_P in Equation 2, the time-independent amplitude of CF decays to the point P on

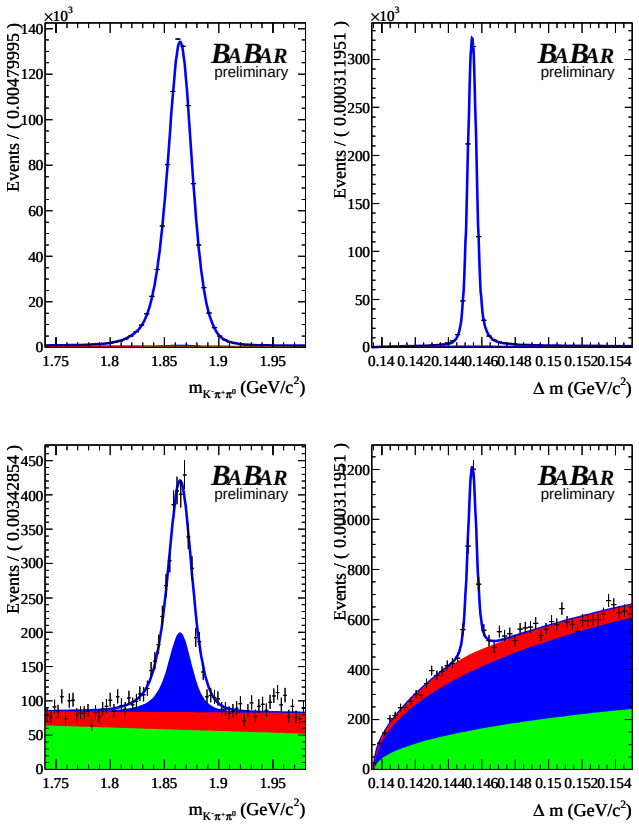

FIG. 5: (Distributions of RS (top) and WS (bottom) data (points with error bars) with fitted PDFs (dashed line) overlaid. The $m_{K\pi\pi}$ distribution (left) requires $0.145 < \Delta m < 0.146\,\mathrm{GeV}/c^2$; the Δm distribution (right) requires $1.85 < m_{K\pi\pi} < 1.88 gevcc$. The white regions represent signal events, the light gray (blue) misassociated $\pi_s^{\pm}$ events, the medium gray (red) correctly associated $\pi_s^{\pm}$ with misreconstructed D^0 events, and the dark gray (green) remaining combinatorial background.

Category	N events (RS)	N events (WS)
Signal	639802 ± 1538	1483 ± 56
Combinatoric	1537 ± 57	499 ± 57
Mistag	2384 ± 57	765 ± 29
Bad D^0	3117 ± 93	227 ± 75

TABLE V: Number of RS and WS events of signal and background in the m_{D^0} and Δm signal region.

the Dalitz plot, by fitting the RS Dalitz plot to an isobar model, using the signal and background fractions obtained in the fit to the $m_{K\pi\pi} - \Delta m$ distribution. The background PDF is empirically determined from the $m_{K\pi\pi} - \Delta m$ sidebands, and its fraction is set to the background fraction derived from the $m_{K\pi\pi} - \Delta m$ fit.

With A_P (or more accurately, the phases and amplitudes for intermediate resonances from which A_P can be calculated) known, we then go on to fit the WS sample simultaneously to the Dalitz plot. We thereby determine

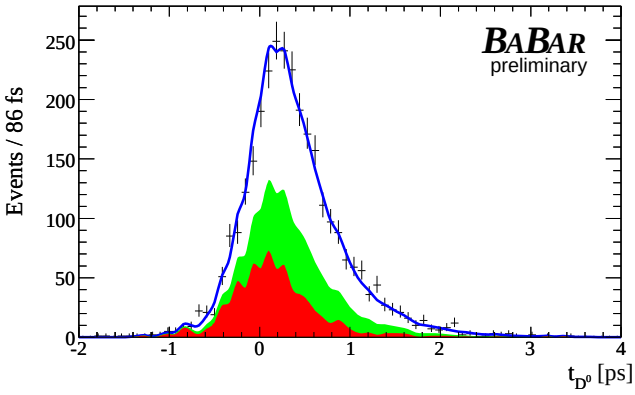

FIG. 6: WS D^0 decay-time distribution (crosses) with fit (solid blue line) overlaid. The green and red regions show the mistag and (combinatoric+bad-D^0) backgrounds respectively. These backgrounds are taken from sideband data, which accounts for their jagged shape.

$\overline{A_P}$, and the decay-time distribution, to extract the mixing parameters. The signal decay-time PDF is taken as Equation 2 convolved with a sum of three Gaussians, as described for the previous two analyses; the parameters of the Gaussians are extracted from a fit to the RS decay-time distribution, and fixed in the WS fit. For the background components, mistagged events are described by the RS parameters, since they contain correctly reconstructed D^0 mesons; the other two background components are described empirically using the sidebands. Figure 6 shows the WS fit projected to the decay time. From this we extract $x'' = 2.39 \pm 0.61$ (stat.) ± 0.32 (syst.)% and $y'' =$ -0.14 $\pm$ 0.60 (stat.) $\pm$ 0.40 (syst.) %. This excludes the no-mixing hypothesis at the 99% confidence level.

$D^0 \to K^+ \pi^- \pi^+ \pi^-$

As in the case of $D^0 \to K^- \pi^+ \pi^0$, the four-body final state $K^+ \pi^- \pi^+ \pi^-$ has a decay-time distribution which varies across the phase space. However, since the phase space is enlarged by one dimension, and the data sample for this analysis is smaller, we do not fit for a decay time at each phase-space point. Instead we integrate across phase space to get a WS to RS decay-rate ratio of

$$\frac{\Gamma_{\mathrm{WS}}(t)}{\Gamma_{\mathrm{RS}}(t)} = \tilde{R}_D + \alpha\tilde{y}'\sqrt{\tilde{R}_D}(\Gamma t) + \frac{1}{4}(\tilde{x}'^2 + \tilde{y}'^2)(\Gamma t)^2 \quad (3)$$

where a tilde indicates integration over phase space. The quantity α is a suppression factor accounting for strong-phase variation across phase space; in effect it measures the amount of information we lose by the integration procedure. As in the $D^0 \to K^- \pi^+$ analysis, $\tilde{R}_D$ is the amplitude for doubly-Cabibbo-suppressed decays, the term

quadratic in time is the amplitude for mixed decays, and the term linear in time is the interference between the two. Again we account for an unknown strong phase by using variables

$$\begin{aligned}\tilde{x}' &= x\cos\tilde{\delta} + y\sin\tilde{\delta} \\ \tilde{y}' &= y\cos\tilde{\delta} - x\sin\tilde{\delta}\end{aligned}$$

where $\tilde{\delta}$ is the strong phase difference integrated across phase space. Equation 3 assumes *CP* conservation. To account for possible *CP* violation in interference between DCS and mixed contributions, we introduce the integrated *CP*-violation phase $\tilde{\phi}$, and parametrise *CP* violation in the mixing itself with $|p/q|$. This allows us to make the substitutions

$$\begin{aligned}\alpha\tilde{y} &\rightarrow |p/q|^{\pm 1}\left(\alpha\tilde{y}'\cos\tilde{\phi} \pm \beta\tilde{x}'\sin\tilde{\phi}\right) \\ \left(x^2+y^2\right) &\rightarrow |p/q|^{\pm 2}\left(x^2+y^2\right)\end{aligned}$$

in Equation 3, applying plus signs for the D^0 sample and minus signs for $\overline{D}^0$. β is an information-loss parameter analogous to α, in this case accounting for phase-space variation in ϕ.

This analysis uses a 230.4 fb^{-1} *BABAR* dataset. The reconstruction procedure is analogous to that of the previous three analyses, the main difference being the requirement that neither pion pair have an invariant mass within 20 MeV/c^2 of the K^0_S mass of 0.4977 GeV/c^2. We demand a D^0 CM momentum requirement of at least 2.4 GeV/c. Two vertex fits are performed, one for the D^0 candidate, required to have a χ^2 probability of at least 0.5%, and one for the full D^* decay tree. For the latter, from which we derive our decay-time value and error, the D^* is constrained to come from the beam-spot, and the probability is required to be at least 1%. The mean σ_t for signal events is 0.29 ps; events with $\sigma_t > 0.5$ ps are rejected. The signal yields are calculated from a fit to the $(m_{K3\pi}, \Delta m)$ distribution; Table VI shows the results.

TABLE VI: Signal yields determined by the two-dimensional fit to the $(m_{K3\pi}, \Delta m)$ distributions for the WS and RS samples. Uncertainties are calculated from the fit.

	D^0	$\overline{D}^0$
WS	$(1.162 \pm 0.053) \times 10^3$	$(1.040 \pm 0.051) \times 10^3$
RS	$(3.511 \pm 0.006) \times 10^5$	$(3.492 \pm 0.006) \times 10^5$

The $(m_{K3\pi}, \Delta m)$ fit which extracts the signal yields also determines shape parameters for those two variables; these are then used in a three-dimensional fit which also includes the time distribution. The decay time function for RS events is a simple exponential convolved with a double Gaussian, with widths proportional to σ_t and separate means. For mistagged events we use the RS decay-time PDF; for mis-reconstructed D^0 component we use the signal PDF; and for combinatorial background a Gaussian with a power-law tail. We fit the RS sample to determine the D^0 lifetime and the time-resolution parameters, which are then held fixed in the fit to the WS sample. We allow yields and background shape parameters to vary. Figure 7 shows the WS decay-time distribution and fit. Figure 8 shows contours of constant likelihood in the (R_D, R_M) plane; we find $R_M = (0.019^{+0.016}_{-0.015} \pm 0.002)\%$ assuming *CP* conservation, and $R_M = (0.017^{+0.017}_{-0.016} \pm 0.003)\%$ with *CP* violation allowed. There is no significant difference between the D^0 and $\overline{D}^0$ samples in the *CP*-allowed fit.

To extract a consistency with the no-mixing hypothesis from these contours is not quite straightforward, because

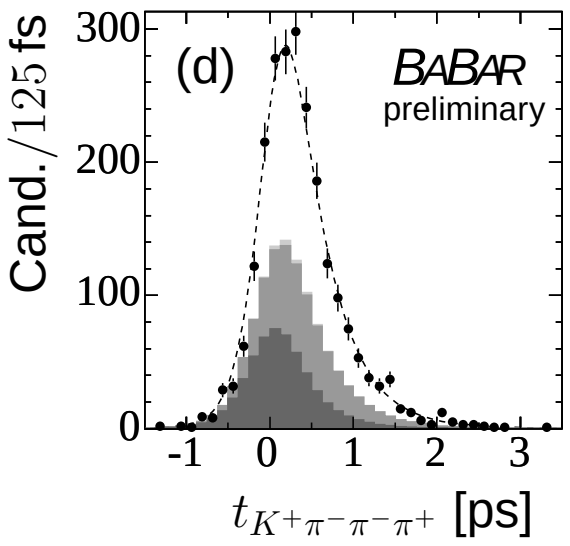

FIG. 7: Distributions of WS data with fitted PDF overlaid. The light gray shows mis-reconstructed charm, the medium gray shows mistagged events, and the dark gray shows combinatorial background.

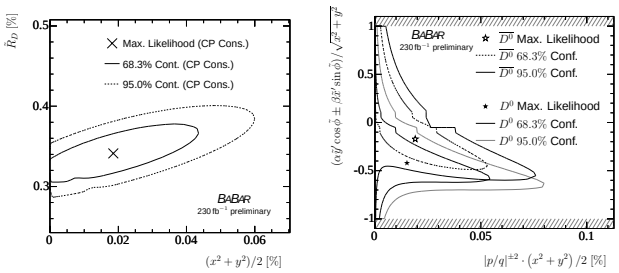

FIG. 8: Left: Contours of constant $\Delta \ln \mathcal{L} = 1.15, 3.0$ in terms of the doubly Cabibbo-suppressed amplitude and the time-integrated mixing rate. Right: Contours of constant $\Delta \ln \mathcal{L} = 1.15, 3.0$ in terms of the normalized interference term and the integrated mixing rate, for the D^0 and $\overline{D}^0$ samples separately. The hatched regions are physically forbidden.

Mode	Luminosity [fb^{-1}]	Mixing	*CP* violation
$D^0 \to K^- \pi^+$	384	3.9 σ	No evidence
$D^0 \to K^- K^+$ or $\pi^+ \pi^-$	384	3.0 σ	No evidence
$D^0 \to K^- \pi^+ \pi^0$	384	Exclude NM at 99% CL	No evidence
$D^0 \to K^- \pi^+ \pi^- \pi^+$	230.4	Consistent with NM at 4.3% CL	No evidence

TABLE VII: Summary of results.

the linear term in Equation 3 becomes unconstrained as R_M approaches zero. We therefore estimate the consistency of our data with no-mixing using a frequentist method; we generate 1000 data sets of 76300 events each, setting the mixing parameters to zero in the generation. We then apply our fit procedure to these sets; in 43 cases we find an R_M equal to or greater than for the data. We therefore conclude that our data are consistent with no-mixing only at the 4.3% confidence level.

We investigate systematic uncertainties from four sources, listed in order of decreasing significance. First is the σ_t threshold, which we increase from 0.5 to 0.6 ps. Second is the decay-time resolution function; we change this by fixing one of the Gaussian widths to be exactly equal to σ_t, letting the other constant of proportionality float as before. Third, the $m_{K3\pi}$ distribution of the background is changed from exponential to a second-order polynomial. And fourth, we use the nominal value of the D^0 lifetime instead of the one obtained from our RS fit. Taken all together, these uncertainties are smaller than the statistical uncertainty by a factor of five.

SUMMARY AND OUTLOOK

BABAR has found evidence for mixing in several channels, as summarised in Table VII. With the total *BABAR* luminosity expected to reach 750 fb^{-1} before shutdown, or nearly twice the largest amount used in these studies, we expect to be able to improve these measurements of the D mixing parameters, and to add other channels as well.

ACKNOWLEDGEMENTS

We are grateful for the excellent luminosity and machine conditions provided by our PEP-II colleagues, and for the substantial dedicated effort from the computing organizations that support *BABAR*. This work is supported by the United States Department of Energy and National Science Foundation.

[1] K. Lande, E. T. Booth, J. Impeduglia, L. M. Lederman, and W. Chinowsky, Phys. Rev. **103**, 1901 (1956);

[2] C. Albajar et al. (UA1 Collaboration), Phys. Lett. **B186**, 247 (1987); H. Albrecht et al. (ARGUS Collaboration), Phys. Lett. **B192**, 245 (1987).

[3] V. M. Abazov et al. (D0 Collaboration), Phys. Rev. Lett. **97**, 021802 (2006); A. Abulencia et al. (CDF Collaboration), Phys. Rev. Lett. **97**, 242003 (2006).

[4] S. Bianco, F. L. Fabbri, D. Benson, and I. Bigi, Riv. Nuovo Cim. **26N7**, 1 (2003); G. Burdman and I. Shipsey, Ann. Rev. Nucl. Part. Sci. **53**, 431 (2003).

[5] L. Wolfenstein, Phys. Lett. **B164**, 170 (1985); J. F. Donoghue, E. Golowich, B. R. Holstein, and J. Trampetic, Phys. Rev. **D33**, 179 (1986); I. I. Y. Bigi and N. G. Uraltsev, Nucl. Phys. **B592**, 92 (2001); A. F. Falk, Y. Grossman, Z. Ligeti, and A. A. Petrov, Phys. Rev. **D65**, 054034 (2002); A. F. Falk, Y. Grossman, Z. Ligeti, Y. Nir, and A. A. Petrov, Phys. Rev. **D69**, 114021 (2004); A. A. Petrov, Int. J. Mod. Phys. **A21**, 5686 (2006).

[6] B. Aubert *et. al.*, (*BABAR* Collaboration), "Evidence for D^0-$\overline{D}^0$ Mixing", submitted to Phys. Rev. Lett, arXiv:hep-ex/0703020v1

[7] B. Aubert *et. al.*, (*BABAR* Collaboration), "Measurement of D^0-$\overline{D}^0$ mixing using the ratio of lifetimes for the decays $D^0 \to K^- \pi^+$, $K^- K^+$, and $\pi^- \pi^+$", submitted to Phys. Rev. D - Rap. Comm.

[8] B. Aubert *et. al.*, (*BABAR* Collaboration), "Search for mixing in $D^0 \to K^+ \pi^- \pi^0$", given at Lepton-Photon 2007.

[9] B. Aubert *et. al.*, (*BABAR* Collaboration), "Search for D^0-antiD^0 mixing in the decays $D^0 \to K^+ \pi^- \pi^+ \pi^-$", given at ICHEP 2006, arXiv:hep-ex/0607090

[10] G. Blaylock, A. Seiden, and Y. Nir, Phys. Lett. **B355**, 555 (1995), hep-ph/9504306.

[11] S. Bergmann, Y. Grossman, Z. Ligeti, Y. Nir, and A. A. Petrov, Phys. Lett. **B486**, 418 (2000), hep-ph/0005181.